Mobility of Adsorbed Proteins Studied by Fluorescence Recovery after Photobleaching

Yonghui Yuan,† Orlin D. Velev,‡ and Abraham M. Lenhoff*

Center for Molecular and Engineering Thermodynamics, Department of Chemical Engineering, University of Delaware, Newark, Delaware 19716

Received August 7, 2002. In Final Form: January 9, 2003

The mobility of proteins adsorbed on a solid substrate and on a lipid monolayer was measured by fluorescence recovery after photobleaching. Both a conventional fluorescence microscope with a charge-coupled device camera and a laser scanning confocal microscope were used. For proteins adsorbed on a solid substrate, the bleached area never recovered fully, while for proteins adsorbed at liquid interfaces, the recovery was very fast. The data analysis to evaluate diffusion coefficients was done on the basis of the full intensity profiles instead of the conventional method based on recovery curves in terms of average or total intensities. The diffusion coefficients were obtained by fitting the experimental data to the intensity profiles calculated based on a solution of the diffusion equation in two dimensions, thereby reducing the possible effects of artifacts in the intensity measurements. The diffusion coefficients at the liquid interface obtained by this method were on the order of 10^{-7} cm^2/s. Comparison with the results for proteins adsorbed on a supported lipid monolayer show that the fast recovery is related to the tangential mobility of the floating lipid monolayer.

Introduction

Extensive research has been performed on the macroscopic scale to probe protein adsorption, particularly in the areas of adsorption kinetics, equilibrium, and relevant transport phenomena for different systems. However, information considering the molecular-level behavior of adsorbed proteins forms a relatively small fraction of this work, and understanding of such issues as lateral mobility, conformation, orientation, and ordering of protein molecules is thus incomplete. It is especially translational mobility of adsorbed protein that we investigate here, which is relevant to such applications as protein transport in chromatography and formation of structured adlayers at surfaces.

Much of the present understanding of the mobility of adsorbed proteins is inferred from observations, generally by scanning probe microscopy (SPM), of the two-dimensional structure of the adsorbed layer. The adsorbed protein molecules are usually found to be randomly distributed,[1−7] but ordering to various degrees has been observed at fluid interfaces such as Langmuir films,[6,8,9] denatured protein films,[10] or the free surface of mercury.[11] The ability of the adsorbed proteins to form ordered structures may be contingent on their lateral mobility. This argument is supported by the observation that streptavidin molecules were found to self-assemble into two-dimensional crystals more quickly at the liquid−vapor interface than on solid-supported lipid layers and on mica.[12] These results suggest that ordering is achieved by initial random adsorption followed by subsequent surface transport, so that self-assembly requires the mobility of the protein molecules to be high enough that they can come together and rearrange on the surface. It can be inferred from this work that the lateral mobility of streptavidin at the liquid−vapor interface is higher than that at the solid−liquid interface, but no study has shown quantitatively the difference in protein mobilities at the two kinds of interfaces.

In this work, we seek to measure the surface mobility of adsorbed protein molecules directly and quantitatively by fluorescence recovery after photobleaching (FRAP). FRAP, also called (micro)photolysis, was first developed as a technique to measure rates of lateral transport of proteins and lipids in cell membranes.[13] It is based on using a high-intensity light beam to destroy permanently the fluorescence of the molecules in the bleaching area. The geometry of the bleached area can be either a spot or parallel stripes (pattern photobleaching, FRAPP). After the bleaching process, the recovery of the fluorescence due to the diffusion of fluorescent molecules from the surrounding unbleached areas into the bleached area is monitored, from which the diffusion coefficient (D) of the fluorescent molecules can be derived.

Details of the numerous FRAP studies of mobility and diffusion are available in the review of Henis.[14] Most studies of mobility have been performed in planar lipid bilayers and on cell membranes;[15,16] these have found that

* To whom correspondence should be addressed. Fax: +1-302-831-4466. E-mail: lenhoff@che.udel.edu.

† Present address: Unilever Research, 45 River Road, Edgewater, NJ 07020.

‡ Present address: Department of Chemical Engineering, North Carolina State University, Raleigh, NC 27695-7905.

(1) Yang, J.; Mou, J.; Shao, Z. *Biochim. Biophys. Acta* **1994**, *1199*, 105−114.

(2) Toulhoat, H.; Prayer, C.; Rouquet, G. *Colloids Surf., A* **1994**, *91*, 267−283.

(3) Gunning, A. P.; Wilde, P. J.; Clark, D. C.; Morris, V. J.; Parker, M. L.; Gunning, P. A. *J. Colloid Interface Sci.* **1996**, *183*, 600−602.

(4) Mori, O.; Imae, T. *Colloids Surf., B* **1997**, *9*, 31−36.

(5) Ortega-Vinuesa, J. L.; Tengvall, P.; Lundström, I. *Thin Solid Films* **1998**, *324*, 257−273.

(6) Johnson, C. A.; Yuan, Y.; Lenhoff, A. M. *J. Colloid Interface Sci.* **2000**, *223*, 261−272.

(7) Yuan, Y.; Oberholzer, M. R.; Lenhoff, A. M. *Colloids Surf., A* **2000**, *165*, 125−141.

(8) Ohnishi, S.; Hara, M.-H.; Furuno, T.; Sasabe, H. *Biophys. J.* **1992**, *63*, 1425−1431.

(9) Ohnishi, S.; Hara, M.-H.; Furuno, T.; Knoll, W.; Sasabe, H. *Mater. Res. Soc. Symp. Proc.* **1993**, *295*, 145−150.

(10) Yoshimura, H.; Scheybani, T.; Baumeister, W.; Nagayama, K. *Langmuir* **1994**, *10*, 3290−3295.

(11) Yamaki, M.; Matsubara, K.; Nagayama, K. *Langmuir* **1993**, *9*, 3154−3158.

(12) Calvert, T. L.; Leckband, D. *Langmuir* **1997**, *13*, 6737−6745.

(13) Axelrod, D.; Koppel, D. E.; Schlessinger, J.; Elson, E.; Webb, W. W. *Biophys. J.* **1976**, *16*, 1055−1069.

(14) Henis, Y. I. *Biomembranes* **1998**, 280−339.

10.1021/la026368m CCC: $25.00
Published on Web 03/15/2003

Table 1. Diffusion Coefficients of Adsorbed Molecules Determined in FRAP Studies

system(s)	method	D (cm^2/s)	reference
BSA on PMMA and PDMS[a]	TIRF−FRAPP	1.2×10^{-9}; 2.6×10^{-9}	17
bovine prothrombin fragment 1 on supported planar membrane	TIRF−FRAPP	10^{-9} on fluidlike membrane; no translational mobility on solidlike membrane	19
antibody on supported lipid monolayer	TIRF−FRAPP	10^{-8}	20
acridine orange on silane-modified silica	FRAPP	$1.3(\pm 0.1) \times 10^{-7}$	21
acridine orange on silane-modified silica	FRAPP	10^{-7} on 100% silane-covered surface; 10^{-9} on 24% covered surface	22
DNA oligonucleotides on APTES-coated glass[b]	TIRF−FRAP, CCD camera	10^{-9}	23
ferritin and lysozyme on solid substrates, lipid monolayers, and transferred lipid monolayers	TIRF, CCD camera	$\ll 10^{-9}$ on solid substrates and transferred monolayers; 4×10^{-7} (ferritin) and 5×10^{-7} (lysozyme) on lipid monolayers	this work

[a] PMMA, poly(methyl methacrylate); PDMS, poly(dimethylsiloxane). [b] APTES, (3-aminopropyl)triethoxy silane.

membrane proteins in living cells typically diffuse at least an order of magnitude more slowly than expected from the lipid bilayer viscosity (relative to lipid lateral diffusion in the same membrane) and significantly more slowly than their diffusion in artificial membranes (10^{-8} cm^2/s). A possible reason is that membrane proteins are anchored to the cytoskeleton.

In more recent studies, the application of FRAP was extended to proteins adsorbed on surfaces, in some cases in combination with total internal reflection fluorescence (TIRF) in order to restrict the fluorescence signal collected to that from molecules near the surface. Representative results of lateral diffusion coefficient measurements on various systems, on both labeled proteins and free fluorophores, and the corresponding methods used are summarized in Table 1. Experiments of this kind have shown that the lateral mobility may be influenced by factors such as differences in surface properties[17] and hindrance due to protein−protein lateral interactions.[18]

In most of the above FRAP studies, data acquisition was by a photomultiplier tube (PMT), which measures the total intensity in a single spot. The diffusion coefficient was obtained by plotting the total fluorescence intensity versus time after bleaching and fitting the intensity change to a diffusion model. This method of measurement does not provide spatially resolved fluorescence intensities, so the data might be unreliable if there is exchange of protein between the surface and the bulk or a change in the excitation light intensity, which would cause shifts in the whole intensity profile. Thus any increases in total intensity resulting from reasons other than lateral diffusion might misleadingly be attributed to lateral diffusion. The effects of such confounding contributions can be ameliorated by a modification of the FRAPP method that employs both the recovery and depletion signals,[24] but full intensity profiles are still not analyzed. These may contain useful information regarding effects such as concentration-dependent or other nonlinear diffusion mechanisms.

In contrast to the PMT, a charge-coupled device (CCD) camera enables the direct visualization of the bleached and unbleached areas as well as measurement of the intensity profiles showing surface mass transfer and fluorescence recovery. The intensity profiles can also be normalized relative to those prior to bleaching. Thus the change in the measurement method can improve the reliability of the FRAP method and reveal nonstandard transport mechanisms by making use of a more complete data set. The approach was first utilized in the video-FRAP approach,[25] in which the sequence of images is analyzed in Fourier space. Measurement of intensity profiles by CCD has also been employed in analyzing the adsorption and surface diffusion of oligonucleotides at the liquid−solid interface.[23] This study mentioned several advantages of using the full profiles but did not use them, while in other cases[26] the intensity profiles were not shown and the diffusion coefficients were not reported. Thus this potential to obtain and analyze the intensity profiles within the microscope field of view has not been fully utilized previously. Spatially resolved intensity data may also be obtained by performing FRAP using scanning confocal fluorescence microscopy,[27] which has the additional advantage of limiting the collected intensity to the focal plane. As a result, it is possible to perform measurements of 2D diffusion even in bulk samples.

In this work, the lateral diffusion of proteins adsorbed on solid−liquid interfaces, floating lipid monolayers, and supported lipid monolayers is compared. The effects of bulk diffusion and protein desorption on the experimental results are discussed. The conventional spot bleaching method was used in the FRAP experiments using either a collimated beam in a conventional fluorescence microscope or the laser in a scanning confocal microscope. The intensity profiles were acquired by a CCD camera, and the diffusion coefficients were obtained by fitting the full experimental intensity profiles to calculated values in real space.

Theory

The lateral diffusion of the adsorbed fluorescent molecules into the bleached area in our experiments can be modeled under the assumptions that all fluorescence recovery is the result of pure two-dimensional diffusion (no flow) in an infinite plane and that no diffusion in or out of the bleached area occurs during bleaching. Using

(15) Fahey, P. F.; Koppel, D. E.; Barak, L. S.; Wole, D. E.; Elson, E. L.; Webb, W. W. *Science* **1977**, *195*, 305−306.
(16) Schlessinger, J.; Axelrod, D.; Koppel, D. E.; Webb, W. W.; Elson, E. L. *Science* **1997**, *195*, 307−308.
(17) Tilton, R. D.; Robertson, C. R.; Gast, A. P. *J. Colloid Interface Sci.* **1990**, *137*, 192−203.
(18) Tilton, R. D.; Gast, A. P.; Robertson, C. R. *Biophys. J.* **1990**, *58*, 1321−1326.
(19) Huang, Z.; Pearce, K. H.; Thompson, N. L. *Biophys. J.* **1994**, *67*, 1754−1766.
(20) Timbs, M. M.; Poglitsch, C. L.; Pisarchick, M. L.; Sumner, M. T.; Thompson, N. L. *Biochim. Biophys. Acta* **1991**, *1064*, 219−228.
(21) Zulli, S. L.; Kovaleski, J. M.; Zhu, X. R.; Harris, J. M.; Wirth, M. J. *Anal. Chem.* **1994**, *66*, 1708−1712.
(22) Kovaleski, J. M.; Wirth, M. J. *J. Phys. Chem. B* **1997**, *101*, 5545−5548.
(23) Chan, V.; Graves, D. J.; Fortina, P.; McKenzie, S. E. *Langmuir* **1997**, *13*, 320−329.
(24) Kim, S.; Yu, H. *J. Phys. Chem.* **1992**, *96*, 4034−4040.
(25) Tsay, T. T.; Jacobson, K. A. *Biophys. J.* **1991**, *60*, 360−368.
(26) Wirth, M. J.; Ludes, M. D.; Swinton, D. J. *Anal. Chem.* **1999**, *71*, 3911−3917.
(27) Blonk, J. C. G.; Don, A.; van Aalst, H.; Birmingham, J. J. *J. Microsc.* **1993**, *169*, 363−374.

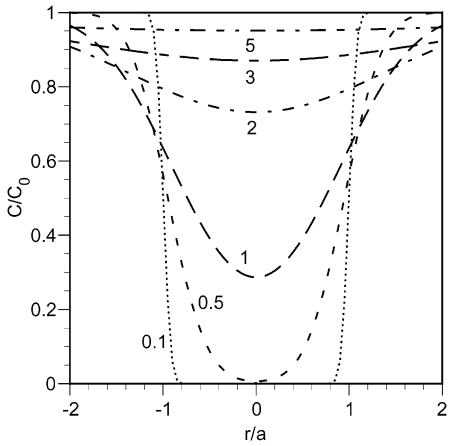

Figure 1. Calculated dimensionless concentration profiles for lateral diffusion from an instantaneous cylindrical source. Labels show dimensionless time $t^* = tD/a^2$.

the solution of the diffusion equation for an instantaneous cylindrical source,[28] the concentration profile C' at time t and position r can be expressed as

$$C' = \frac{1}{2Dt}\exp\left(-\frac{r^2}{4Dt}\right)\int_0^a \exp\left(-\frac{r'^2}{4Dt}\right) I_0\left(\frac{rr'}{2Dt}\right) r'\,\mathrm{d}r' \quad (1)$$

Here I_0 is the modified Bessel function of the first kind of order zero, and a is the radius of the bleached spot. The calculated radial concentration profiles for different times postbleaching, expressed in dimensionless terms as $t^* = (Dt/a^2)^{1/2}$, are plotted in Figure 1. At short times ($t^* < 1$), the profiles change markedly and the curves move inward. For $t^* \gg 2$, however, diffusion spreads the bleached molecules beyond their original confined region and the curves are much flatter, so the shape change is not as obvious as when $t^* < 1$. In our experiments, we obtained a set of intensity profiles that were fitted to concentration curves calculated by eq 1 using a least-squares method to estimate the diffusion coefficient D. However, by performing the analysis in real space we can fit the intensity profiles directly to any postulated diffusion model.

Materials and Methods

Experimental Setup. In the conventional fluorescence microscope setup, an Olympus BH2-RFL reflected light fluorescence attachment on an Olympus BHT microscope was used. Blue light (wavelength, 350−500 nm) obtained from a mercury exciter with a B (BP-490) filter was used for both bleaching and data collection. Before the experiment, the mercury light source of the microscope was adjusted to ensure that the field of view was illuminated as symmetrically and uniformly as possible so that the beam intensity was uniform inside and outside the bleaching spot.

Emitted fluorescence was collected by a Star I/IEEE-488 cooled CCD camera (Photometrics). The picture of the sample surface was seen on a monitor and also transferred to a Macintosh computer using IP Lab Spectrum software. Images were stored in memory at different time intervals to monitor the recovery of the intensity in the bleached area. The horizontal intensity profiles were obtained by a cross-sectional analysis of the pictures, usually by averaging the intensity of a column of eight or nine pixels.

The confocal microscope bleaching and imaging data were collected on a Zeiss 510 LSM confocal microscope with a 30 mW ArKr laser source (488 nm). The objective was a 63× C-Apochromat (numerical aperture, 1.2) water-immersion lens, and the bleaching was performed by scanning the laser at high intensity across a 50 μm diameter circular disk, using the bleaching function of the microscope software.

Protein Labeling. Lysozyme and ferritin were obtained from Sigma-Aldrich (St. Louis, MO), and fluorescein 5-isothiocyanate (FITC) was obtained from Molecular Probes (Eugene, OR). The labeling was carried out by the procedure provided by the latter company.[29] After the labeling reaction, the protein and the free dye were separated by size exclusion chromatography in a 10 × 300 mm Sephadex G-25 column. The buffer was 5 mM phosphate and 2 mM sodium azide, pH 6.5. The collected protein was stored at 4 °C for future use. The labeling ratios were close to 1 in all cases, as determined by UV−vis spectroscopy.[29]

Sample Preparation. For the FRAP experiments with proteins adsorbed on solid surfaces, the solid was freshly peeled mica or an aminosilane-coated glass slide for lysozyme or ferritin, respectively. The silane was trimethoxysilylpropyldiethylenetriamine (DETA, from United Chemical Technologies, Bristol, PA). The glass coverslips, 15 mm in diameter, were from Ted Pella, Inc. (Redding, CA). The glass was modified as described previously.[6] To prepare the sample for FRAP, a drop of solution of fluorescently labeled protein (0.1 mg/mL) was placed on the solid surface for 20 min, then rinsed off with deionized water, and finally replaced by a drop of a comparable solution of unlabeled protein. An imaging chamber (20 mm diameter, 1 mm deep; Sigma-Aldrich) was used to cover both the solid substrate and the solution droplet. The top of the droplet was in contact with the top of the chamber, thereby facilitating microscopic observation.

Viewing proteins on a lipid monolayer is complicated by the mobility of the liquid−air interface, which allows the bleached area to float out of the field of view if the surface area is not small enough. Therefore a small and shallow chamber must be used to reduce the drift. The sample also has to be sealed in order to prevent air flow that can cause the liquid interface to move and to prevent water evaporation that can dry the sample, especially when very little water is used. The lipids, 1,2-dipalmitoyl-*sn*-glycero-3-phosphocholine (DPPC) and 1,2-dipalmitoyl-*sn*-glycero-3-(phospho-l-serine)(sodium salt) (DPPS) from Avanti Polar Lipids (Alabaster, AL), were dissolved in chloroform in a ratio of 4:1 to form a 12.5 mg/mL solution. Phosphate buffer solution (0.5 mL) was placed in an imaging chamber (20 mm diameter, 2.5 mm deep; Sigma-Aldrich), and then 5 μL of lipid−chloroform solution was placed on the buffer interface using a syringe. After the chloroform had evaporated and the monolayer was spread on the aqueous solution, 100 μL of lysozyme or ferritin solution (1 mg/mL) was injected into the subphase using another syringe. The adsorption time allowed was 30 min. The imaging chamber was covered by a glass coverslip (Fisher Scientific, Pittsburgh, PA) to prevent evaporation. Great care was needed to control the depth of the buffer in the imaging chamber so that the meniscus of the buffer would not touch the coverslip but the sample would still be within the working distance of the objective lens.

The corresponding FRAP experiments using a confocal microscope with an inverted stage used a 63× water-immersion objective lens, and since the working distance is only about 200 μm, the thickness of the subphase film had to be less than that. Since so little subphase liquid was used, the evaporative thinning of the liquid film could allow the monolayer to touch the glass slide. Evaporation would stop eventually due to saturation of the cell with vapor, but controlling the thickness of the liquid film remained difficult. The focus also had to be readjusted during the experiments due to the lowering of the interface.

Experiments were also conducted with protein adsorbed on transferred lipid monolayers. In this case, 32 or 54 μL of lipid−chloroform solution was first spread on a Langmuir−Blodgett trough (model 1000DE minitrough, KSV Instruments, Helsinki, Finland), and the surface pressure was measured by a platinum Wilhelmy plate. The monolayer was then transferred to a silane-coated glass coverslip (15 mm diameter) by the "touching" method at surface pressures of 3 and 40 mN/m. The adsorption and further sample preparation were the same as in the first paragraph of this section.

FRAP Protocol. After protein adsorption had been allowed to occur, a picture of the sample was taken as background using

(28) Crank, J. *The Mathematics of Diffusion*, 2nd ed.; Clarendon Press: Oxford, 1975.

(29) *Conjugation with Amine-Reactive Probes*; Product Information Sheet; Molecular Probes: Eugene, OR, 1998.

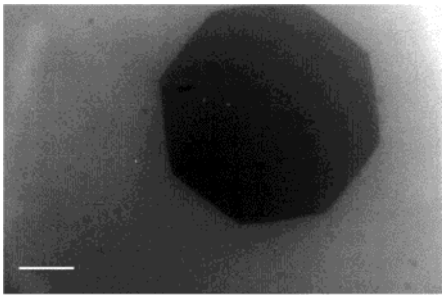

Figure 2. Typical fluorescence image, after bleaching, of proteins adsorbed on a solid substrate. Scale bar, 50 μm.

a 10× objective before bleaching. The intensity profile from this picture was used to normalize the later intensity profiles to account for the effect of the profile inhomogeneity of the excitation source. The field diaphragm was then closed to the smallest diameter, and the shutter was fully opened to allow passage of high-intensity light. A 20× objective was used for the bleaching. The bleached area is octagonal, with a diameter of approximately 200 μm (Figure 2). The bleaching times were varied depending on the sample, to achieve adequate contrast, and are given in the figure captions for each data set.

After the bleaching, the shutter was returned to the low-pass mode. The diaphragm was opened, the objective was changed back to the 10× one, and the focus was readjusted. Pictures were taken at appropriate adaptive time intervals, usually shorter at the beginning and longer at later times. The mercury lamp was turned off only if no picture was going to be taken in the next hour. The lamp was turned on for at least 20 min before each measurement to stabilize the intensity of the excitation beam.

FRAP experiments could be performed much more conveniently using the "bleach" function of the confocal microscope. The bleached area can be any shape, and the switching from imaging to bleaching mode is computer-controlled. Pictures can be taken immediately after the bleaching is finished, and this was done automatically every 12.5 s.

Data Processing and Curve Fitting. A series of intensity profiles were obtained for each experiment and fitted to the calculated concentration profiles to obtain the diffusion coefficient. Since the intensity profiles shift with time, both horizontally and vertically, these offsets have to be accounted for during curve fitting. The lateral shifts were found from the minimum points of the curves. The vertical shift of the intensity profiles, which was not considered in most previous studies, was obtained by a least-squares fitting of the experimental data with the offset included as an independent adjustable parameter for each intensity profile.

Results and Discussion

Solid Interfaces. FRAP profiles for ferritin on silane-coated glass and lysozyme on mica are shown in Figure 3. In both cases, the intensity profiles have essentially the same shapes throughout the first 2 h after photobleaching. However, there is an intensity increase with time in both data sets, which in the first hour is much smaller for ferritin than for lysozyme. Because the supernatant solution contained unlabeled protein, even additional adsorption of protein would not have caused the intensity increase. A likely explanation for this trend is adsorption of labeled protein from the bulk, with desorption of adsorbed protein outside the bleached area providing a source of additional labeled protein. The smaller and slower increase for ferritin would be due to its larger size (diameter of ca. 12.5 nm, compared to ca. 4 nm for lysozyme). The adsorption of ferritin would be expected to be much stronger and essentially irreversible,[6] so there would be less likelihood of exchange of adsorbed ferritin. For lysozyme, on the other hand, more adsorbed labeled lysozyme could be expected to desorb into the buffer solution and later readsorb, causing the intensity increase.

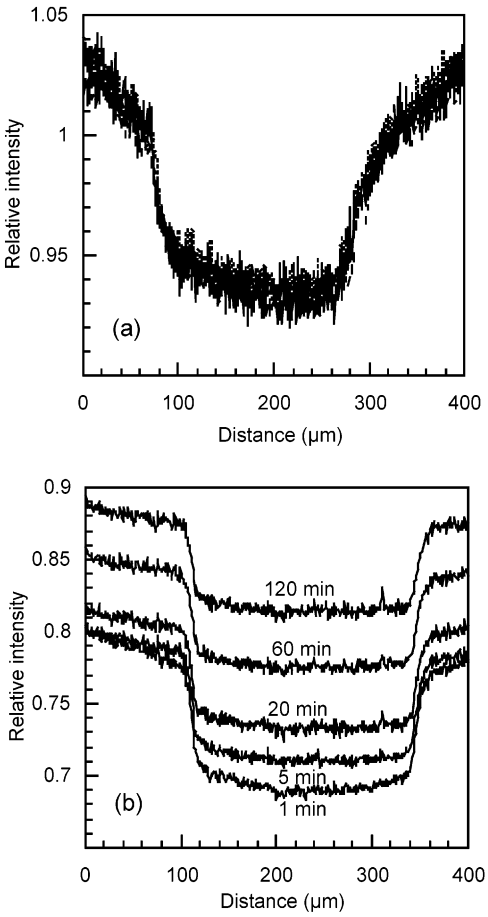

Figure 3. Fluorescence intensity profiles for FITC-labeled proteins adsorbed on solid substrates from 1 mM phosphate-buffered saline (PBS), pH 6.5. (a) Ferritin on silane-coated glass. Adsorption time, 40 min; equilibration time with unlabeled ferritin, 40 min; bleaching time, 3 min. Curves are shown for 2 min, 10 min, 51 min, and 2 h after the end of bleaching and are not clearly resolved, but show a consistent but small increase with time. (b) Lysozyme on mica. Adsorption time, 30 min; equilibration time with unlabeled lysozyme, 30 min; bleaching time, 15 min.

Additional control experiments indicated that the labeling procedure also affected the intensity change. There is an optional reaction quenching step in the procedure after the conjugation reaction.[29] We found that if the proteins used in the adsorption experiments were labeled by the procedure without the quenching step, the intensity would keep increasing even if the bleaching was not carried out and the solution in contact with the sample was replaced with unlabeled lysozyme; however, adding the quenching step in the labeling procedure would reduce the intensity increase.

Independent of its cause, the observed increase in intensity with time clearly shows the pitfall of using only the average intensity to calculate diffusion coefficients, as that approach would lead to misleading conclusions. In our data analysis, we consider only the shapes of the intensity profiles to estimate lateral diffusion rates by comparison with theoretical calculations. Comparison with Figure 1, in which the calculated concentration profiles change appreciably in shape, indicates that there is no significant lateral diffusion in this system, that is, the diffusion coefficient is too small to be detected. Experiments of longer duration showed no evidence of lateral diffusion in 24 h, so that since $Dt/a^2 \ll 1$, the lateral diffusion coefficient $D \ll a^2/t \sim 10^{-9}$ cm^2/s.

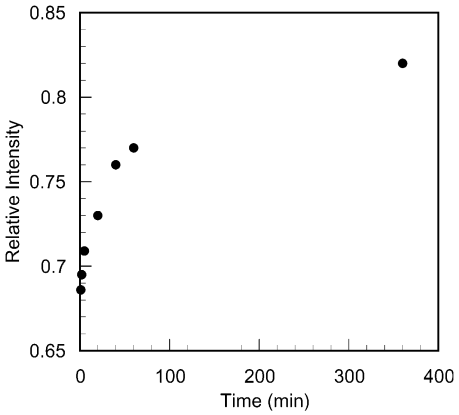

Figure 4. Fluorescence recovery curve for FITC-labeled lysozyme adsorbed on mica, calculated from data in Figure 3b for analysis by the conventional FRAP method.

A further illustration of the potentially misleading interpretations possible using the conventional FRAP measurement of averaged intensity is obtained by applying such an analysis to our results by averaging the intensity in the bleached area numerically and plotting its change with time. Figure 4, which shows the results for lysozyme adsorbed on mica, displays the kind of monotonic increase usually observed; the lateral diffusion coefficient calculated by the Axelrod et al.[13] method is on the order of 10^{-9} cm^2/s. A diffusion coefficient of this magnitude would correspond to largely complete recovery in the bleached area, with the edge of the bleached zone not clearly identifiable. This is not observed in our experiments, in which the fluorescence picture of the sample still shows a very sharp edge after 45 h of recovery.

FRAP experiments were also conducted for ferritin and lysozyme adsorption without preliminary exposure to unlabeled protein; the intensity profiles are shown in Figure 5. In the ferritin experiments, the intensity profiles again barely change in shape, but the full curves move upward slightly with time. For lysozyme, in contrast, the intensity profile in the bleached area immediately after bleaching is curved and that just outside slopes gently. Both these regions level out after about 20 min, and the full profiles move up noticeably.

There are two possible explanations for the changes in the intensity profiles at short times. The first is that only a fraction of the adsorbed protein is mobile, as suggested by measurements of bovine serum albumin (BSA) adsorbed on polymer films.[17] Second, bulk diffusion may contribute to the partial recovery of fluorescence in the experiments on the conventional fluorescence microscope, where the incident light is essentially unattenuated on passing through the surface, so that the protein in the bulk can contribute to fluorescence and can also be bleached. The focal depth of the conventional microscope lens used was of order 10 μm. The emission collected by the objective lens comes from throughout the specimen, including above and below the focal plane. Thus the emission from the bulk close to the focal plane can be collected and contribute to the intensity too. The characteristic time for bulk diffusion can be estimated as $t \sim a^2/D \sim 100$ s. Diffusion in the bulk from the surrounding solution would cause the intensity profile to move upward for dimensionless times of >1, similarly to what is seen in Figure 1. The slope of the profiles would change too, as in both Figure 1 and Figure 5.

This explanation based on bulk bleaching and diffusion is supported by the corresponding experiments performed using the confocal scanning laser microscope (CSLM).

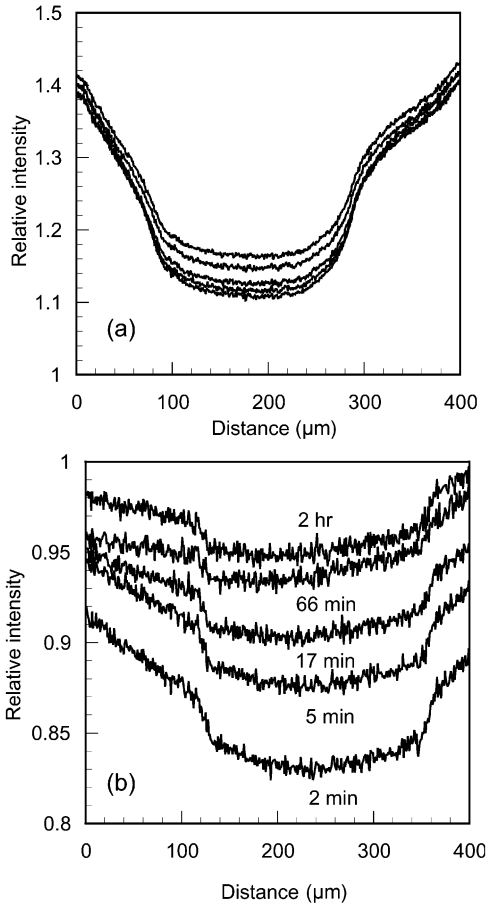

Figure 5. Fluorescence intensity profiles for FITC-labeled proteins adsorbed on solid substrates from 1 mM PBS, pH 6.5, without equilibration with unlabeled protein. (a) Ferritin on silane-coated glass. Adsorption time, 40 min; bleaching time, 10 min. Curves are shown for (from bottom) 5, 10, 20, 60, and 120 min. (b) Lysozyme on mica. Adsorption time, 30 min; bleaching time, 10 min.

Here, the laser beam still passes through the solution, but since the focal depth is much smaller, the beam is tightly focused to a single spot on the surface, greatly attenuating the intensity in the bulk and reducing bleaching of bulk protein. The intensity that is measured comes only from a layer about 0.5 μm thick at the surface, since only light in the focal plane can pass through the pinhole and be collected. Thus the contribution from bulk diffusion is much smaller in the confocal microscopy experiments. The results of the CSLM experiment on lysozyme for the first 20 min after photobleaching are shown in Figure 6. Here the bleached region is initially flat and remains so. However, the profiles still move upward slightly, probably as a result of additional adsorption of labeled lysozyme from the bulk. In contrast to Figure 5b, though, there is no change in the shape of the profiles, which in the absence of a contribution from the bulk indicates that the recovery is not due to lateral diffusion of the adsorbed protein.

Fluid Interfaces. The intensity profiles for lysozyme and ferritin adsorbed at the lipid/water interface (Figure 7) show distinct changes in shape similar to those in the theoretical curves in Figure 1, on time scales of minutes. The recovery was very fast, with the edge of the bleached region and the well-like shape of the profile not seen even in the first picture taken after bleaching. Thus some recovery occurred during bleaching, and the recovery process was substantially complete after about 10 min.

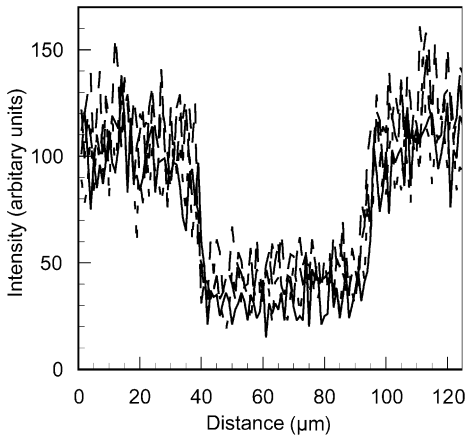

Figure 6. Confocal microscopy fluorescence intensity profiles for FITC-labeled lysozyme adsorbed on mica from 1 mM PBS, pH 6.5. Adsorption time, 30 min; bleaching time, 2 min. Curves are shown for 250, 500, 1000, and 1550 s after the end of bleaching and are all essentially superimposed.

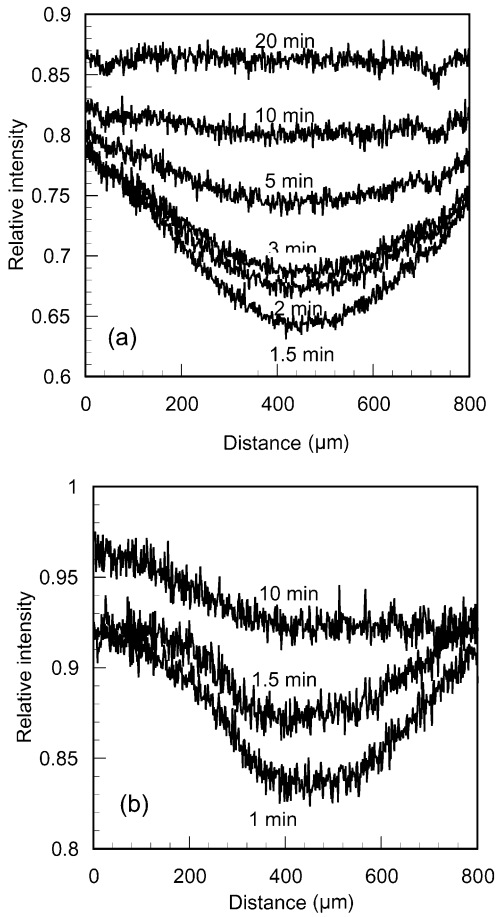

Figure 7. Fluorescence recovery curves for FITC-labeled proteins adsorbed on a floating DPPC−DPPS monolayer. Subphase, 1 mg/mL labeled protein in 1 mM PBS, pH 6.5; monolayer, 25% DPPS + 75% DPPC, surface pressure 3 mN/m; adsorption time, 30 min; bleaching time, 5 min. (a) Ferritin. (b) Lysozyme.

Corresponding experiments were conducted by confocal microscopy as well. For the reasons discussed under Materials and Methods, the lipid monolayer could come in contact with the glass coverslip as the water evaporated. Whereas the monolayer would usually drift slowly on the subphase surface, it stopped floating when it touched the coverslip. The FRAP observations showed that the bleached area did not recover during the observation period

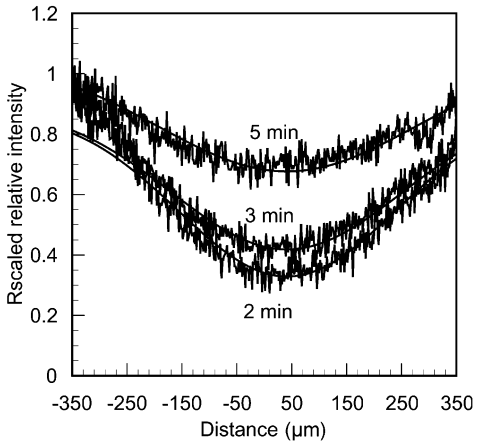

Figure 8. Comparison of rescaled experimental intensity profiles for ferritin adsorbed on a lipid monolayer with the calculated concentration profiles for $D = 5 \times 10^{-7}$ cm^2/s.

(∼1 h) if the monolayer became immobilized on the glass, but that it did so very quickly otherwise.

Estimates of the diffusion coefficients of the adsorbed proteins obtained by fitting the calculated concentration profiles to the experimental data gave diffusion coefficients of 5×10^{-7} cm^2/s for ferritin and 4×10^{-7} cm^2/s for lysozyme. A comparison of the experimental intensity profiles and the theoretically calculated concentration curves for ferritin is shown in Figure 8. The diffusivities of both proteins are fairly high, within an order of magnitude of bulk diffusion coefficients (1.12×10^{-6} cm^2/s for lysozyme and 3.61×10^{-7} cm^2/s for ferritin). The ferritin diffusion coefficient is slightly higher than that of lysozyme, which is a counterintuitive result, as the Stokes−Einstein relation suggests that the lysozyme diffusivity should be higher by about a factor of 3, which is approximately consistent with the bulk values given above. There are two possible reasons for the discrepancy. First, the apparent diffusion coefficient may decrease with the fractional surface coverage,[18] and since lysozyme is positively charged, it may be expected to adsorb more readily on the negatively charged lipid than ferritin, which is negatively charged. Second, lysozyme may form aggregates, as was shown by atomic force microscope imaging of lysozyme on mica,[30] so its effective size on the surface may be larger than the molecular dimensions.

The diffusivity values are also higher in absolute terms than results obtained in previous experiments of this kind (Table 1). Although bulk diffusion may have contributed partially to the observed diffusion behavior, the available theoretical models of diffusion in two dimensions also provide a basis for more variability in 2D diffusion coefficients than is the case for 3D diffusion. The theory of Brownian motion of particles in membranes[31] shows that translational diffusivities in two dimensions can be very large, approaching infinite values for a membrane of infinite extent. The lateral diffusion coefficient for a particle of radius a at the center of a circular membrane of radius R ($R \gg a$) with viscosity μ is given by

$$D = \frac{kT}{4\pi\mu h}\left(\log\frac{R}{a} - \frac{1}{2}\right) \qquad (2)$$

where h is the thickness of the membrane. This equation does not describe the exact conditions of our experiments,

(30) Radmacher, M.; Fritz, M.; Cleveland, J. P.; Walters, D. A.; Hansma, P. K. *Langmuir* **1994**, *10*, 3809−3814.
(31) Saffman, P. G.; Delbrück, M. *Proc. Natl. Acad. Sci. U.S.A.* **1975**, *72*, 3111−3113.

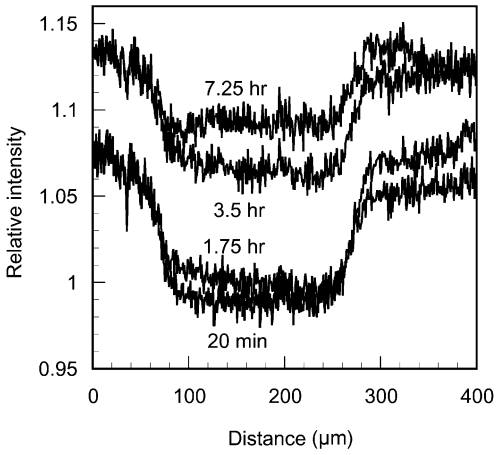

Figure 9. Fluorescence recovery curves for lysozyme adsorbed on a transferred DPPS−DPPC monolayer. Solution, 1 mg/mL lysozyme in 1 mM PBS, pH 6.5; monolayer, 25% DPPC + 75% DPPS, surface pressure 3 mN/m; adsorption time, 30 min; bleaching time, 3 min.

but it can still provide some indication of predicted trends. For example, for ferritin in a water "membrane" of radius 1 cm and thickness 12.5 nm, D is calculated to be about 8.5 times the bulk diffusion coefficient. Related observations of Brownian motion of a particle floating at the air−water interface were made by Radoev et al.[32] The diffusion coefficient was expressed as

$$D = \frac{kT}{6\pi\mu a f(h/a)} \tag{3}$$

where the factor $f(h/a)$ depends on the vertical position of the particle at the interface. For a pendant sphere fully immersed in liquid, f was found to be 0.716, so that the diffusion coefficient is 1.4 times the bulk value. Although theoretical results for the specific system of proteins adsorbed on a floating lipid monolayer are not available, the above studies imply that a lateral diffusion coefficient higher than or close to the bulk diffusion coefficient is possible.

Several sources of uncertainty during the experiments limit the accuracy with which the diffusion coefficients can be estimated. These include the partial recovery during the bleaching period, the time taken for adjusting the instrument between bleaching and imaging due to the change in the objective lens, and the diffraction of light by the edge of the shutter, which causes the edge of the bleached region to be fuzzy. As discussed in the previous section, bulk diffusion may contribute to the observed change in the intensity profiles, so the value of the diffusion coefficient may have been overestimated. These factors, taken together, result in values for the estimated diffusion coefficients of ferritin and lysozyme that are similar within the bounds of experimental uncertainty. However, the results clearly prove that recovery on fluid interfaces is orders of magnitude more rapid than on solid interfaces. This recovery is related to the interfacial mobility of the proteins, as bulk diffusion alone is not enough to explain the fast recovery at the fluid interfaces.

Supported Lipid Monolayers. FRAP experiments were also performed with lysozyme adsorbed on the same lipid monolayer used above, but after it had first been transferred onto a solid substrate. The profiles obtained (Figure 9) are very similar to those of lysozyme adsorbed on mica. Even after more than 7 h, there is little change in the shape of the intensity profiles, and lateral diffusion is not observed. Since adsorption/desorption should be comparable on the free and supported monolayers, the profound difference in FRAP behavior between these two cases clearly shows that the fast recovery observed at the fluid interface is caused not by desorption of the adsorbed protein but by fast lateral diffusion.

Parameter Estimation Methodology. The methodology used here for comparing, normalizing, and fitting the full recovery profiles has allowed extraction of a set of data that we believe reliably reflects the true physical processes taking place. The experiments have displayed a number of artifacts that may affect results obtained by the conventional pattern bleaching and averaged intensity measurements. First, our methodology revealed and accounted for significant shifts in intensity caused by continuing protein adsorption from the bulk, without the use of wide-field spot photobleaching.[23] Such drifts in the overall signal for any reason can be revealed most directly by acquisition of the full recovery profiles, such as described previously in the video-FRAP method.[25] However, real space rather than Fourier space analysis is more versatile in that it allows consideration of nonlinear effects.

Second, we have shown that artifacts can be introduced by bleaching and diffusional recovery from the nonadsorbed protein in the liquid adjacent to the surface. This effect can be minimized by implementing the method in TIR or on a confocal microscope,[27] thereby restricting the depth of the bleached layer. Thus, it appears that the most precise FRAP results on protein surface mobility can be obtained by a combination of TIR or confocal microscopy and full profile fitting. We anticipate that further improvement of that specific technique can not only produce precise and reliable data, but can also capture subtler nonlinear and cooperative diffusion effects that have not been measured reliably to date.

Conclusions

The FRAP experimental results (Table 1) show that proteins adsorbed at the lipid−water interface have much higher mobilities than those adsorbed at the solid−liquid interface, because of the mobile character of the lipid monolayer itself. It is clear from our experiments that diffusion of proteins adsorbed on the free lipid monolayer and on a solid surface, even on a supported lipid monolayer, is very different. Rapid fluorescence recovery occurred only on the free lipid monolayer, demonstrating that the mobility of the lipid monolayer is critical to the mobility of the adsorbed proteins. Even if adsorption is strong, the adsorbed protein molecules can move with the lipid molecules, and this surface mobility leads to the high effective diffusion coefficients seen on the free monolayers.

A more general conclusion is that the traditional method of data analysis for FRAP experiments, that is, the recovery curve method, is not appropriate under conditions in which effects other than lateral Fickian diffusion at the interface of interest might contribute to the intensity change. Intensity increases originating from bulk diffusion, additional adsorption from the bulk, and environmental changes would lead to misleading estimates of the diffusion coefficients using this method. Measurement of the full profiles, particularly when using confocal microscopy and multiphoton microscopy, can improve the reliability of FRAP experiments.

Acknowledgment. We are grateful for support from the NSF (Grant Number CTS-9977120) and NASA (Grant Number NAG8-1242).

LA026368M

(32) Radoev, B.; Nedjalkov, M.; Djakovich, V. *Langmuir* **1992**, *8*, 2962−2965.